

Water Absorption, Mechanical, and Crystallization Properties of High-density Polyethylene filled with Corncob Powder

Shiliu Zhu,^a Yong Guo,^{a,*} Daowu Tu,^a Yuxia Chen,^a Shengquan Liu,^{a,*} Wei Li,^b and Li Wang^a

Corncob powder filled high-density polyethylene (HDPE) composites were prepared by extrusion. The microstructure, water absorption, mechanical properties, and crystallinity of composite at different corncob powder content were investigated. Results demonstrated that when the corncob powder levels were moderate and uniformly dispersed within the HDPE matrix, the powder acted as a reinforcing agent. As the corncob content increased, the water absorption of the resulting composite gradually increased, which adversely affected the composite's water resistance. Flexural strengths and moduli initially increased with increasing corncob powder levels, and then consequently decreased at higher powder levels; maximum values for flexural properties were achieved at 40% corncob powder content. The composite's impact strength and toughness weakened with corncob powder addition. The X-ray diffraction and differential scanning calorimetry analyses indicated that when the corncob content increased, the peak crystallization and melting temperatures of the matrix increased and decreased, respectively. Meanwhile, the presence of the corncob restricted the movement and arrangement of the HDPE polymer chains, which affected HDPE crystal growth and causing a decrease in crystallinity.

Keywords: Corncob powder; High-density polyethylene (HDPE); Composites; Crystallinity; Mechanical properties

Contact information: a: Department of Forest Products Industry, Anhui Agricultural University, Hefei 230036, China; b: Department of Suzhou Dongda Wood Industry Co., Ltd, Suzhou 234101, Anhui, China; Corresponding authors: fly828828@163.com (Yong Guo) and liusq@ahau.edu.cn (Shengquan Liu)

INTRODUCTION

Research of renewable and recyclable resources derived from biomasses has received increased attention to address the depletion of non-renewable petrochemical resources. China is a large agricultural country that has abundant biomass resources that are available at low costs (Tingyun *et al.* 2007). These biomass resources can be used to prepare wood-plastic composites (WPCs).

WPCs are a more environmentally sustainable material, which utilize biomass resources. At present, the reinforcing agents utilized for the preparation of wood-plastic composites include: wood and bamboo fibers (Zakikhani *et al.* 2014; Ansari *et al.* 2017); jute, hemp, and flax fibers (Bledzki *et al.* 2015; Haag *et al.* 2017; Sullins *et al.* 2017); agriculture straw and forestry waste fibers (Leão *et al.* 2015; Cisneros-López *et al.* 2017); rice husks (Aridi *et al.* 2016); and walnut and hazelnut shells (Ayrilmis *et al.* 2013; Tufan and Ayrilmis 2016). Ashori and Nourbakhsh (2010) extensively studied the effects of hot-water treatment and particle sizes of fibers, which were obtained from various wood species, on select physical and mechanical properties of WPCs. Panthapulakkal *et al.* (2006) investigated the mechanical properties of polypropylene composites that contained 30% wheat straw fibers, as well as the effects of chemical treatments of these

fibers. Wheat straw fiber reinforced polypropylene composites exhibited significantly enhanced properties compared to virgin polypropylene. However, the strength properties of the composites were less for chemically prepared fiber filled composites. The mechanical, thermal, thermo-mechanical, and dynamic properties of PLA/HSF (poly(lactic acid)/hazelnut shell flour) composites with various compositions have been studied by Balart *et al.* (2016). Faruk *et al.* (2012) examined several variables of biomass-plastic composites, which included the fiber types, the environmental conditions, the processing methods, and the fiber modifications; the authors reported that these variables have complex interactions relative to the impact on the performance of the resulting composite.

Corncoobs are a by-product waste of corn processing. It is a promising biomass resource in China due to its high abundance and stable availability. The National Bureau of Statistics of the People's Republic of China indicated that corn production is approximately 200 million tons a year, which affords corncob annual yields around 40 to 50 million tons. In the past, corncobs were regarded as agricultural waste by farmers, and they were used as fuel or for composting. These disposal methods greatly underutilize this biomass resource. But as technology develops, corncobs are starting to be used in biological feed, industrial raw materials, edible fungi, and energy. Much research has been conducted on alternative usages for corncobs. At present, most of this work has focused on its use for the production of xylose (Deng *et al.* 2016; Yan *et al.* 2017), furfural (Liu *et al.* 2017; Zhang *et al.* 2017), activated carbon (Qu *et al.* 2015), nanocrystalline cellulose (Silvério *et al.* 2013; Ditzel *et al.* 2017), and various nanocomposites (Guo *et al.* 2015; Mao *et al.* 2015). However, a high amount of residue and waste water produced in the preparation process of xylose, furfural, and other chemical products, cause environmental pollution. In addition, the post-treatment consumes a high amount of energy and manpower. However, the use of corncob resources to fabricate WPCs is the realization of green production, and contributes to finding sustainable ways to utilize this waste.

Theoretically, corncob is a typical non-wood fiber material with an average mass composition of 35% to 40% hemicelluloses, 17% to 20% lignin, and 32% to 36% cellulose, in addition to a low amount of inorganic ash (Xu 2011). This indicates that the main components of corncob are similar to wood fiber, which makes it is entirely possible to produce wood-plastic composite. For instance, Luo *et al.* (2017) found that corncob was the more suitable corn fiber for the preparation of corn fiber plastic composites; and the mechanical properties of the composites were affected by the composition in terms of the cellulose, hemicellulose, and lignin fractions. A high cellulose and lignin content improved the mechanical properties, whereas a high hemicellulose would decrease the water resistance and mechanical properties. Panthapulakkal and Sain (2007) studied the surface chemistry and thermal degradation characteristics of corncob fiber to demonstrate the effect of surface chemistry on the end use properties of the composites and the practicability of processing it with thermoplastics. Furthermore, the viability of corncob as reinforcements in HDPE was evaluated as compared to wheat straw and cornstalk. In addition, composites composed of LDPE, PVC plastisol, and different amounts of untreated and pre-treated ground corncob were prepared, and the physical and mechanical properties was studied as compared to the composites filled with eucalyptus wood and brewery's spent grain (Georgopoulos *et al.* 2005). In these studies, the difference between the corncob and other plant fibers was dominated, and most of them remained in the laboratory stage and the standard splines by injection molding were mainly used, and there was no upper pilot line or production line. In addition, the mechanical properties of the composites in these studies need further improvement to meet practical application requirements and a

comprehensive feasibility analysis is required, including the materials, formula, preparation method, compounding mechanism and product performance. In order to save costs and efficient use of the waste corncob, a high-filled corncob composite is required. Therefore, the authors selected the corncob powder (CP) to prepare corncob powder filled HDPE (CP-HDPE) composites and studied the water absorption, mechanical properties, and crystallization properties of the composites. Furthermore, this experiment was carried out on a pilot-scale production line, which was based entirely on the production mode of existing factories. The results can be directly extended to the actual production of the factory. It will provide important research and production data on the utilization of this non-wood biomass for the production of plastic composites.

EXPERIMENTAL

Materials

Corn cob powder (CP) with an average particle size of 180 μm was purchased from Yanggu Ruikang Technology Co., Ltd. (Yanggu, China). The particle size distribution of CP is shown in Table 1, which is based on the mass fraction. High-density polyethylene (HDPE; grade: 5000S; the melt flow index (MFI) is 0.9 g/10 min) was obtained from Dongguan Baoyu Plastic Materials Co., Ltd. (Dongguan, China). Lubricant (Westrchem STR-530, recommended for wood flour / fiber-filled polyethylene (PE) systems) and compatibilizer (maleic anhydride grafted polyethylene (MA-g-PE)) were obtained from Shanghai Guangyu Chemical Co., Ltd. (Shanghai, China). Figure 1 shows the corn and its byproducts.

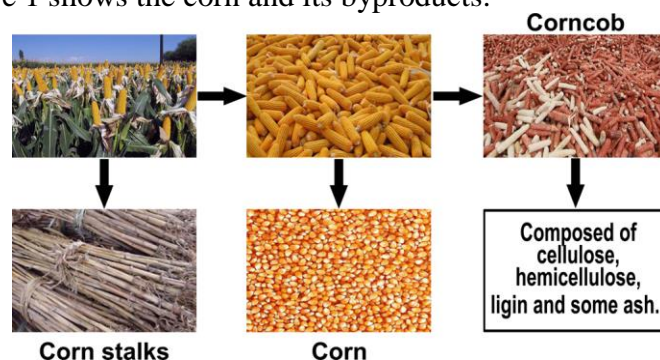


Fig. 1. Corn and its byproducts

Table 1. Corncob Powder Particle Size Distribution

Particle size	<150 μm	150–180 μm	180 μm	180–250 μm
mass fraction%	6.4	13.8	74.1	5.7

Methods

Manufacturing of corncob powder filled HDPE composites

The formulated composites and their corresponding designations are presented in Table 2. The corncob powder was dried prior to its use (dried at 103 $^{\circ}\text{C}$ for 24 h), and had a moisture content of less than 2% (by mass). The required amounts of CP, HDPE, and other additives were blended together in accordance to the formulations of Table 2 in a high-speed mixer (model:

SHR-25A; Zhangjiagang Jiahua Plastic Machinery Co., Ltd. (Zhangjiagang, China)) for 20 min at 80 °C; the speed of the rotor is 1200 r/min. Among them, the amount of lubricant (Westrchem STR-530) and compatibilizer (MA-g-PE) is 2% of the total amount of corncob powder and HDPE, respectively. The blended mixture was pelletized with a granulator (model: SWMSZ-S1; the L/D (length to diameter) ratios is 40; Nanjing Sky Win Technology Co., Ltd. (Nanjing, China)). The pelletizer had temperature profiles of 150, 180, 180, 175, and 160 °C for the five temperature zones, and operated with a screw rotation speed of 400 rpm. The resulting pellets were added to a second single screw extruder (model: SWMSD-S1; L/D =30; Nanjing Nanjing Sky Win Technology Co., Ltd. (Nanjing, China)), which operated with the temperature profiles 135, 145, 150, 155, and 155 °C for the five temperature zones and a screw rotation speed of 6 rpm. The extruded material was injected into a mold at a temperature of 140 °C. Figure 2 illustrates the process schematic for fabricating the composites.

Table 2. Formulated CP-HDPE Composites and Their Designations

Sample Designation	Corncob Powder (%)	HDPE (%)	MA-g-PE (%)	STR 530 (%)
30% CP-HDPE	30	70	2	2
40% CP-HDPE	40	60	2	2
50% CP-HDPE	50	50	2	2
60% CP-HDPE	60 </td <td>40</td> <td>2</td> <td>2</td>	40	2	2
70% CP-HDPE	70	30	2	2

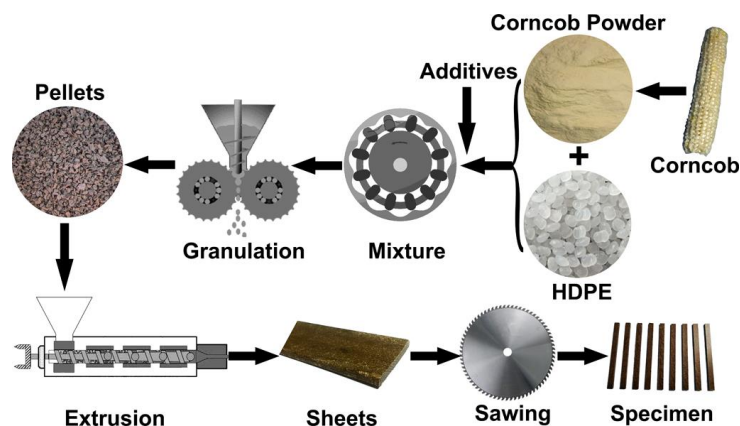


Fig. 2. Schematic of the fabrication process of CP-HDPE composites

Characterization

Scanning electron microscopy (SEM) was performed using a Hitachi S-4800 microscope (Tokyo, Japan). The SEM operated with an accelerating voltage of 1.0 kV. The impact fractured surfaces of the composite samples were coated with a thin layer of gold prior to the SEM analysis (Kaewtatip and Thongmee 2012; Dikobe and Luyt 2017).

X-ray diffraction (XRD) analyses of the composites were obtained utilizing a MSAL XD-3 X-ray diffractometer (Beijing Purkinje General Instrument Co., Ltd. (Beijing, China)). The instrument used $\text{CuK}\alpha$ radiation ($\lambda = 1.5406 \text{ \AA}$; 36 kV; and 20 mA) to scan the samples at a rate of $1^\circ/\text{min}$; samples were scanned over the range of $2\theta = 5^\circ$ to 80° . The data was processed by MDI Jade 6.0 software and the crystallite size was calculated from the Scherrer formula (Babiker *et al.* 2010),

$$D = K\lambda/\beta\cos\theta \quad (1)$$

where D is the crystallite size, K is Scherrer constant ($K=0.89$), β is the full width at half maximum, and θ is the diffraction angle.

Differential scanning calorimetry (DSC) analyses of the CP-HDPE composites were performed using a DSC 200F3 differential calorimeter (Netzsch, Germany), which was fitted with a liquid nitrogen cooling system. The heating and cooling steps were conducted under a N_2 atmosphere. Samples were heated from $-25\text{ }^\circ\text{C}$ to $200\text{ }^\circ\text{C}$ using a heating rate of $10\text{ }^\circ\text{C}/\text{min}$, then held at $200\text{ }^\circ\text{C}$ for 5 min (to eliminate the thermal history), then cooled to $25\text{ }^\circ\text{C}$ using a cooling rate of $5\text{ }^\circ\text{C}/\text{min}$, and finally heated again to $200\text{ }^\circ\text{C}$ using a heating rate of $10\text{ }^\circ\text{C}/\text{min}$ (Hristov and Vasileva 2003). The amount of sample used during the DSC scans was between 5 and 7 mg. Samples were hermetically sealed in a DCS device prior to being placed into the instrument. The crystallization (T_c) and melting (T_m) temperatures were determined during crystallization and endothermic melting, respectively, whereas the heat of fusion (ΔH) was calculated from the peak area of the DCS thermogram. The degree of crystallinity (X_c) was calculated from the DSC thermogram using the following expression (Hristov and Vasileva 2003),

$$X_c = \Delta H/\Delta H_0 \times 100\% \quad (2)$$

where ΔH is the heat of fusion of the CP-HDPE composite (J/g), and ΔH_0 is the heat of fusion of 100% crystalline HDPE, which is taken to be 293 J/g according to Na *et al.* (2002).

Physical and mechanical properties

Water absorption tests were conducted with $50\text{ mm}\times 50\text{ mm}\times 5\text{ mm}$ sized samples and determined in accordance to Chinese standard GB/T 1462-2005 “Test Methods for Water Absorption of Fiber Reinforced Plastics.” Adsorption tests were replicated five times; reported values for the samples were the averages from the replicates. The specimens were oven-dried at $50 \pm 2\text{ }^\circ\text{C}$ for 24 h, which was then cooled to room temperature in a desiccator; the conditioned mass of the specimen (W_1) was measured with an accuracy of $\pm 0.001\text{ g}$. The test specimen was then immersed in a container of distilled water at room temperature ($23 \pm 1\text{ }^\circ\text{C}$) for 24 h. Afterwards, the test specimen was carefully dried with a dry cloth and the wet mass (W_2) was determined immediately to the nearest 0.001 g . The soaked sample was oven-dried at $50 \pm 2\text{ }^\circ\text{C}$ for 24 h, and then cooled to room temperature in a desiccator; the mass of the soaked sample after drying and conditioning (W_3) was measured. The absolute water absorption of the specimen (W_a) was determined by the following equations:

$$\begin{aligned} W_a &= W_2 - W_3 \quad (\text{if } W_3 < W_1) \\ W_a &= W_2 - W_1 \quad (\text{if } W_3 > W_1) \end{aligned} \quad (3)$$

The percentage increase in specimen mass (W) during water immersion was calculated as:

$$W = W_a/W_1 \times 100\% \quad (4)$$

Three point flexural tests (sample size: $120\text{ mm}\times 10\text{ mm}\times 5\text{ mm}$) and Charpy un-notched impact tests (sample size: $80\text{ mm}\times 10\text{ mm}\times 5\text{ mm}$) were measured using a universal testing machine (model: AG-Xplus; Shimadzu, Tokyo, Japan) and a simple beam impact testing machine (model: XJJ-50; Chengde Juyuan Testing Equipment Manufacture Co., Ltd., Chengde, China), respectively, in accordance to Chinese standards GB/T 9341-2008 (“Plastics – Determination of Flexural Properties”) and GB/T 1043.1-2008 (“GB/T 1043.1-2008 Plastics – Determination of Charpy Impact Properties – Part 1: Non-Instrumented Impact Test”).

Mechanical test were repeated ten times and the reported values are the averages of the replicates average.

RESULTS AND DISCUSSION

Interfacial Morphology

Figure 3 depicts the typical fracture surface images from the SEM analyses of the CP-HDPE composites, where: (a) and (b) correspond to 30% CP-HDPE; (c) and (d) correspond to 40% CP-HDPE; and (e) and (f) correspond to 70% CP-HDPE. As shown in Fig. 3(a), the corncob powder was heterogeneously distributed within the HDPE matrix as small pockets (*i.e.*, “island” shapes) when the corncob powder substitution levels were low (*i.e.*, 30%). The image shows apparent pores caused by poor compatibility, and it was easy to distinguish the interphase between the corncob powder and the HDPE. By contrast, the distribution area of the corncob powder was apparently increased, and the powder was well coated by the HDPE matrix (Fig. 3(c) and 3(d)). The interface interaction enhanced between the corncob powder and the HDPE, and the interface diffusion and mechanical interlocking effects improved. As the corncob powder substitution level increased above 70% in the composites, its distribution throughout the HDPE matrix became more heterogeneous (Fig. 3(e), (f)). The corncob powder exhibited an agglomeration effect and accumulated on the HDPE matrix due to the intermolecular effect of hydroxyl groups. The interfacial interaction between corncob powder and HDPE matrix is weakened and the compatibility is poor. From these observations, it was apparent that an optimum substitution level of corncob powder content existed where the fibers and HDPE matrix had intimate contact and mechanical interlocking. In these circumstances, the interfaces between the two phases were strong.

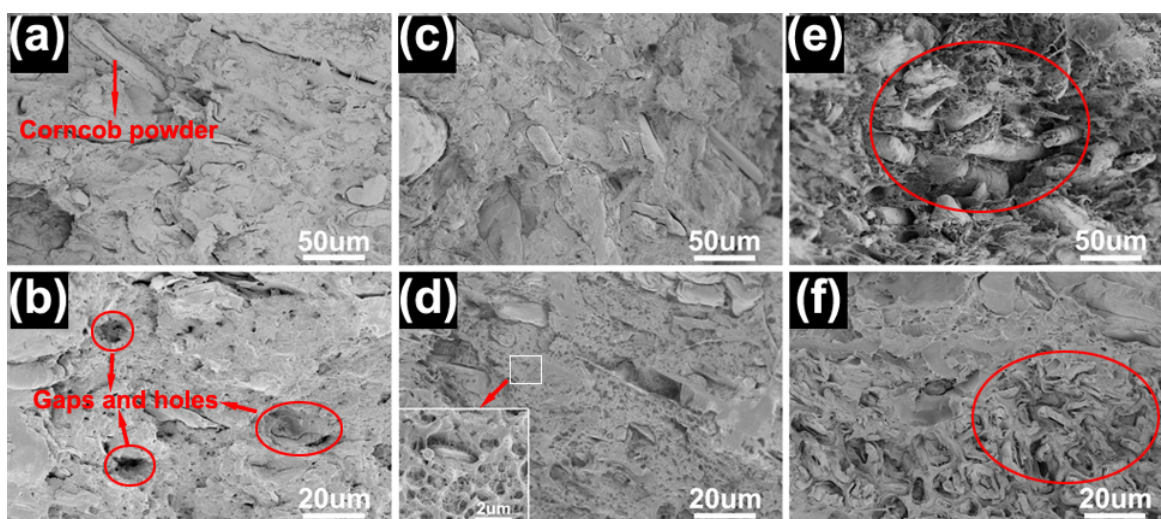


Fig. 3. SEM images of fractured surfaces CP-HDPE composites from impact tests from: (a) and (b) 30% CP-HDPE; (c) and (d) 40% CP-HDPE; (e) and (f) 70% CP-HDPE

Water Absorption

Water absorption is one of the most important characteristics of a WPC; it dictates the dimensional stability of the composites, and it ultimately determines its application in outdoor environments. The water absorption of the WPC is mainly determined by the lignocellulosic

fiber content and the interfacial compatibility of the phases of the composites. The lignocellulosic fibers are mainly composed of cellulose, hemicelluloses, and lignin. Some of these components have a high number of polar hydroxyl groups distributed on the surface, which can easily form hydrogen bonds with water molecules (Aquino *et al.* 2007). Water molecules can easily access the open pores of the interfaces between the corncob powder and the HDPE, which is attributed to poor fiber-HEDP matrix compatibility. The results from water absorption tests of CP-HDPE composites are presented in Table 3. As the corncob powder mass fraction increased from 30% to 50%, the water absorption of the composites gradually increased. The water absorption of the composites reached the maximum value of 0.93%, when the corncob powder content was 70% (70% CP-HDPE), which was much higher when compared to 30% CP-HDPE (30% corncob powder). However, the water absorption of CP-HDPE composites was lower than the 3.00% standard and the previous studies on corncob reinforced plastics (Panthapulakkal and Sain 2007; Luo *et al.* 2017).

Under the same preparation conditions, the water absorption of the composite mainly depended upon the lignocellulosic fiber substitution level. The higher the lignocellulosic fiber substitution levels were, the more the composite adsorbed water; this could be attributed to higher amounts of cellulose and hemicelluloses in the composite, which have hydroxyl groups that interact with water molecules through hydrogen bonding (Aquino *et al.* 2007). These observations are consistent with various literature reports (Adhikary *et al.* 2008; Nourbakhsh and Kouhpayehzadeh 2009). Hence, the water resistances of composites with high corncob powder substitution levels are poor. Furthermore, high corncob powder substitution levels led to a deteriorated dispersion, and produce a lot of interface defects. Pores were created at the interfaces of the two phases, which formed channels for water molecules to enter into the composites (Stokke and Gardner 2003).

Table 3. Water Absorption of Composites with Different Formulations

Sample	Absolute Water Absorption (g)	Water Absorption	95% Confidence Interval
30% CP-HDPE	0.0276 ± 0.0028	0.25% ± 0.02%	(0.23%, 0.27%)
40% CP-HDPE	0.0379 ± 0.0040	0.35% ± 0.03%	(0.32%, 0.38%)
50% CP-HDPE	0.0456 ± 0.0060	0.41% ± 0.05%	(0.37%, 0.45%)
60% CP-HDPE	0.0858 ± 0.0048	0.73% ± 0.04%	(0.70%, 0.76%)
70% CP-HDPE	0.1030 ± 0.0252	0.93% ± 0.22%	(0.69%, 1.16%)

Mechanical Properties

Flexural properties

Table 4 presents the flexural properties of the CP-HDPE composites.

Table 4. Flexural Properties of CP-HDPE Composites

Sample	Flexural Strength (MPa)	95% Confidence Interval (MPa)	Flexural Modulus (MPa)	95% Confidence Interval (MPa)
Neat HDPE	24.78 ± 1.43	(23.00, 26.56)	1346.20 ± 47.57	(1287.14, 1405.26)
30% CP-HDPE	44.47 ± 2.13	(42.95, 45.99)	2402.48 ± 92.08	(2325.50, 2479.47)
40% CP-HDPE	57.17 ± 2.96	(54.90, 59.45)	4064.13 ± 94.89	(3946.31, 4181.96)
50% CP-HDPE	52.39 ± 2.02	(50.95, 53.84)	3472.80 ± 68.64	(3420.04, 3525.56)
60% CP-HDPE	49.23 ± 1.50	(48.16, 50.31)	3607.77 ± 82.67	(3548.63, 3666.90)
70% CP-HDPE	43.14 ± 0.56	(42.74, 43.54)	2731.58 ± 52.27	(2683.23, 2779.92)

The results showed that the flexural strengths and flexural moduli of the composites increased as the corncob powder content increased from 30% to 40%, reaching the maximum values of 57.2 MPa and 4064.1 MPa, respectively (40% CP-HDPE); afterwards, these strength properties generally decreased as the corncob powder content increased above 40%. When 40% CP-HDPE was compared to 30% CP-HDPE, the increase in flexural strength and modulus was 28.6% and 69.2%, respectively.

In general, the strength of wood-plastic composites mainly depends on the corresponding composition, such as the strength of the lignocellulosic fibers and the plastic matrix, as well as the interfacial bonding strength between the components (Das and Chakraborty 2006, 2008). Under the same matrix and preparation process, the mechanical strength of the composite is determined by the lignocellulosic fiber strength. The hemicellulose and lignin have significant effects on all properties of corn fiber plastic composites, and high cellulose and lignin content improved its mechanical properties. The highest flexural strength and tensile break strength were achieved with the highest cellulose content as the reinforcement (Luo *et al.* 2017). In addition, the lignin content of the corncob was high and the presence of lignin increased the interfacial compatibility of the corncob and HDPE matrix. Therefore, the corncob powder plays a strengthening role in the complex system, and the flexural properties of composites initially increased with the increase in corncob powder content and then decreased as the powder content continued to grow, a result also reported in the literature (Yali 2012). When the corncob powder substitution level is low, the powder is unevenly distributed within the HDPE matrix, forming small pockets or “islands.” This type of powder distribution resulted in localized stress concentration levels at the stress damaged site (Nenkova *et al.* 2006; Song *et al.* 2013). However, the interfacial bonding between the corncob powder and HDPE matrix is poor when the powder content is very high, which is due to ineffective HDPE coating of the powder. In addition, the coupling agent is a more important factor relative to the flexural properties (Yali 2012); and the amount of MA-g-PE is too low to effectively promote compatibility with the HDPE matrix and the corncob powder, resulting in a decrease in flexural properties. The corncob powder was evenly distributed within the plastic matrix when the powder substitution level was moderate; this resulted in good phase-to-phase interface compatibility that afforded good strength properties. The above composite strength observations were consistent with the observations from SEM analyses.

Impact strength

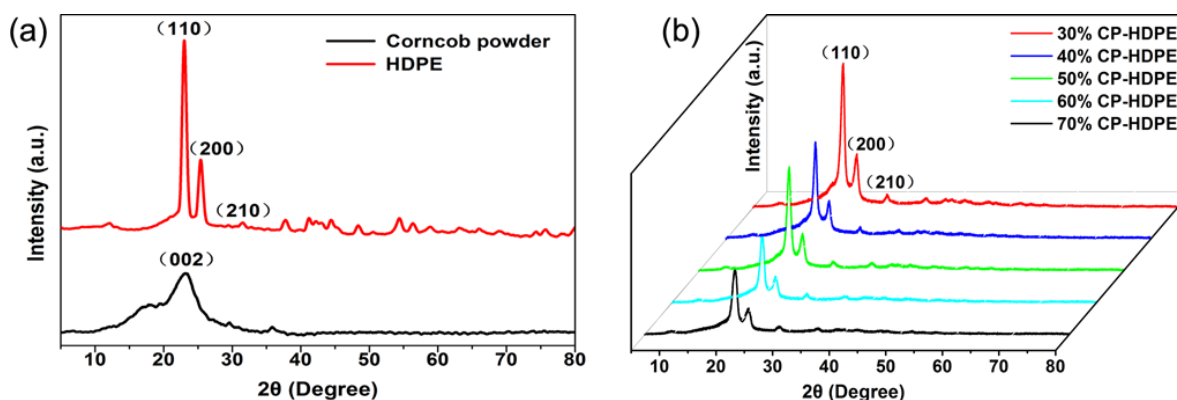
The impact strengths of various samples are presented in Table 5. As the corncob powder content increased, the impact strength gradually decreased. The impact strength was decreased by 45.6% when 70% CP-HDPE was compared to 30% CP-HDPE. The addition of corncob powder disrupted the continuity of the HDPE matrix, which inhibited the absorption and energy transmission when a force was applied; this resulted in lower resistance to deformation. Furthermore, the more severe damage to the resin phase continuity resulted from the higher powder substitution level. The powder acts as a stress-triggered point under transient forces, causing the composite to expand and break instantaneously (Li and Wolcott 2006; Song *et al.* 2013).

Table 5. Charpy Unnotched Impact Strengths of CP-HDPE Composites

Sample	Impact Strength (kJ/m ²)	95% Confidence Interval (kJ/m ²)
30% CP-HDPE	19.86 ± 0.68	(19.02, 20.72)
40% CP-HDPE	15.65 ± 1.26	(14.08, 17.23)
50% CP-HDPE	15.95 ± 0.49	(15.34, 16.55)
60% CP-HDPE	10.49 ± 0.40	(9.99, 10.99)
70% CP-HDPE	10.80 ± 0.20	(10.55, 11.05)

X-Ray Diffraction

Figure 4 presents the XRD analyses of the corncob powder, HDPE, and CP-HDPE composites with various percentages of the corncob powder. The main diffraction angle (2θ), full width at half maximum (β), and crystallite size (D) of the HDPE and CP-HDPE are shown in Table 6. The characteristic diffraction peaks for the HDPE at 2θ were 22.95° (110), 25.38° (200), and 31.48° (210) and did not change when the corncob powder levels in the composite formulation changed. These results indicated that the addition of corncob powder did not change the crystal form of the HDPE, as it always belonged to the orthorhombic lattice (Kang *et al.* 2001; Qiao *et al.* 2009; Zhu and Yang 2010). In contrast, as the corncob powder content increased, the intensity corresponding to each characteristic diffraction peak was appreciably reduced, whereas the half-width gradually increased. The crystallinity of the composites was apparently reduced; the grain size was lower, whereas the crystal growth was imperfect. This might be ascribed to the introduction of corncob powder to the matrix, which disrupted the ability of the polymer strands to orient themselves in an orderly fashion, resulting in the decreased crystallinity of the HDPE.

**Fig. 4.** X-ray diffractions of (a) corncob powder and HDPE, (b) CP-HDPE composites

DSC Analysis

Figure 5 displays the DSC curves of the CP-HDPE composites. It was observed that there was only one melting peak and one crystallization peak during the heating and cooling curves, respectively, with the various composites. This observation indicated that the crystal formation in the composite system was relatively simple and no new crystal forms appeared. These results were consistent with the findings from the XRD analyses. Furthermore, the peak intensities were significantly different. The initial melting temperature (T_{im}), the peak melting temperature (T_{pm}), the end melting temperature (T_{em}), the melting enthalpy (ΔH_m), the initial crystallization temperature (T_{ic}), the peak crystallization temperature (T_{pc}), the end crystallization temperature

(T_{ec}), the crystallization enthalpy (ΔH_c), and the crystallinity (X_c) of the melting, as well as the crystallization curves, are given in Tables 7 and 8.

Table 6. The Diffraction Angle (2θ), Full Width at Half Maximum (β), and Crystallite Size (D) of the HDPE and CP-HDPE

Sample		(110)	(200)	Sample		(110)	(200)
HDPE	2θ (°)	22.946	25.384	50% CP-HDPE	2θ (°)	20.795	23.109
	β (°)	0.666	0.658		β (°)	0.764	0.747
	D (nm)	12.047	12.249		D (nm)	10.464	10.744
30% CP-HDPE	2θ (°)	20.890	23.287	60% CP-HDPE	2θ (°)	20.781	23.097
	β (°)	0.717	0.687		β (°)	0.791	0.756
	D (nm)	11.152	11.686		D (nm)	10.107	10.616
40% CP-HDPE	2θ (°)	20.809	23.197	70% CP-HDPE	2θ (°)	20.779	23.064
	β (°)	0.726	0.734		β (°)	0.822	0.803
	D (nm)	11.012	10.936		D (nm)	9.725	9.994

Table 7. Characteristic Data of CP-HDPE Composites in Melting Curve

Sample	T_{im} (°C)	T_{pm} (°C)	T_{em} (°C)	ΔH_m (J·g ⁻¹)
30% CP-HDPE	125.00	137.90	145.50	222.90
40% CP-HDPE	124.40	136.80	143.30	144.90
50% CP-HDPE	124.30	134.30	139.90	80.02
60% CP-HDPE	123.90	133.30	138.90	65.02
70% CP-HDPE	124.10	132.90	137.70	50.20

Table 8. Characteristic Data of CP-HDPE Composites in Crystal Curve

Sample	T_{ic} (°C)	T_{pc} (°C)	T_{ec} (°C)	ΔH_c (J·g ⁻¹)	X_c (%)
30% CP-HDPE	121.50	116.40	107.70	229.30	76.07
40% CP-HDPE	121.50	116.90	109.10	144.20	49.47
50% CP-HDPE	121.50	118.20	112.00	81.83	27.31
60% CP-HDPE	121.30	118.50	113.00	60.60	22.19
70% CP-HDPE	121.00	118.20	113.40	44.68	17.13

From Table 7, it was apparent that the peak melting temperature and melting enthalpy of the composites decreased as the corncob powder content increased. The T_{pm} decreased from 137.9 °C (30% CP-HDPE) to 132.9 °C (70% CP-HDPE), and the corresponding ΔH_m decreased from 222.9 J·g⁻¹ to 50.2 J·g⁻¹. This was mainly attributed to the dilution effect of the powder within the HDPE matrix (Amash and Zugenmaier 2000), which affected the melting of the HDPE. The results presented in Table 8 indicated that the T_{pc} of the composites increased slightly as the corncob powder content increased. This result demonstrated that the corncob powder played a role of heterogeneous nucleation in the HDPE matrix and further increased the T_{pc} of the HDPE (Bouafif *et al.* 2009; Huang *et al.* 2015). In contrast, the X_c and ΔH_c of the composites were appreciably reduced. The molecular polymer segments were rearranged during the crystallization process, whereas the viscosity of the polymer increased as the corncob powder content increased. Therefore, the motions of the HDPE polymer segments were restricted, which resulted in noticeable reductions in the X_c and ΔH_c values.

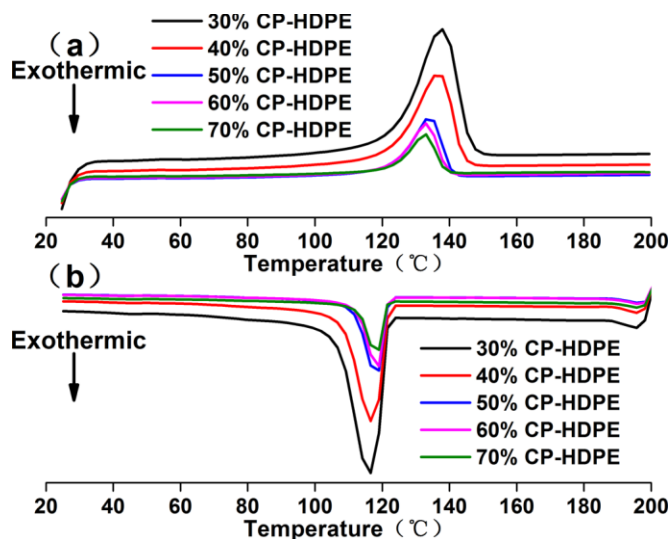


Fig. 5. DSC curves of CP-HDPE composites: (a) melting and (b) crystallization curve

CONCLUSIONS

1. The water resistance of the CP-HDPE composites decreased as the corncob powder content increased based on the experimental results.
2. The flexural properties of the composites increased with the introduction of corncob powder, and they reached the maximum values when the mass fraction of the corncob powder was 40%. This suggested that the corncob powder acted as a reinforcing agent. The experimental results also demonstrated as the substitution levels of corncob powder in the composites increased, the impact strength properties of the material decreased.
3. Results analyses demonstrated that the melting temperature decreased, whereas the crystallization temperature increased, as the corncob powder substitution level increased. It is noteworthy that the crystalline form of HDPE did not change as the corncob powder content increased. In contrast, the presence of the powder restricted the movement and arrangement of the HDPE polymer chains to a certain extent, which affected HDPE crystal growth and lowered the degree of crystallinity of the matrix.
4. In order to obtain the best performance of reinforced-polymer composites with corncob powder, the powder substitution level should be between from 40% to 50%. Surface modification of the corncob powder should be considered in a subsequent investigation. It was noteworthy that the dispersion and reinforcing mechanisms of the corncob powder within the polymer matrix, as well as the powder substitution levels, appreciably affected the physical properties of the resulting CP-HDPE composites.

ACKNOWLEDGMENTS

The authors gratefully acknowledge the Major projects of science and technology in Anhui province (16030701087), the Provincial Natural Science Foundation of Anhui

(1708085MC56), the Postdoctoral Science Foundation of China (2014M560503), and the Key Projects of Provincial Natural Science Foundation of Universities in Anhui Program (KJ2016A220) for their financial support. The authors also thank Jun Zhang and Jian Hu for their help and assistance with conducting the experiments.

REFERENCES CITED

- Adhikary, K. B., Pang, S., and Staiger, M. P (2008). "Long-term moisture absorption and thickness swelling behaviour of recycled thermoplastics reinforced with *Pinus radiata* sawdust," *Chem. Eng. J.* 142(2), 190-198. DOI: 10.1016/j.cej.2007.11.024
- Amash, A., and Zugenmaier, P. (2000). "Morphology and properties of isotropic and oriented samples of cellulose fibre–polypropylene composites," *Polym.* 41(4), 1589-1596. DOI: 10.1016/S0032-3861(99)00273-6
- Ansari, F., Granda, L.A., Joffe, R., Berglund, L.A., and Vilaseca, F. (2017). "Experimental evaluation of anisotropy in injection molded polypropylene/wood fiber biocomposites," *Compos. Part A - Appl. Sci. Manuf.* 96(May 2017), 147-154. DOI: 10.1016/j.compositesa.2017.02.003
- Aquino, E., Sarmiento, L., Oliveira, W., and Silva, R. (2007). "Moisture effect on degradation of jute/glass hybrid composites," *J. Reinf. Plast. Compos.* 26(2), 219-233. DOI: 10.1177/0731684407070030
- Aridi, N., Sapuan, S., Zainudin, E., and Al-Oqla, F. M. (2016). "Mechanical and morphological properties of injection-molded rice husk polypropylene composites," *Int. J. Polym. Anal. Charact.* 21(4), 305-313. DOI: 10.1080/1023666X.2016.1148316
- Ashori, A., and Nourbakhsh, A. (2010). "Reinforced polypropylene composites: Effects of chemical compositions and particle size," *Bioresource Technol.* 101(7), 2515-2519. DOI: 10.1016/j.biortech.2009.11.022
- Ayrlimis, N., Kaymakci, A., and Ozdemir, F. (2013). "Physical, mechanical, and thermal properties of polypropylene composites filled with walnut shell flour," *J. Ind. Eng. Chem.* 19(3), 908-914. DOI: 10.1016/j.jiec.2012.11.006
- Babiker, M. E., Zhang, S., Tang, Y. F., and Wang, G. (2010). "The effect of gel and pressure induced flow (PIF) processing conditions on the dispersion and intercalation of MMT nanoclay in UHMWPE/ montmorillonite (MMT) clay based nanocomposite sheets," *International Journal of Chemistry* 2(2). DOI: 10.5539/ijc.v2n2p102
- Balart, J., Fombuena, V., Fenollar, O., Boronat, T., and Sánchez-Nacher, L. (2016). "Processing and characterization of high environmental efficiency composites based on PLA and hazelnut shell flour (HSF) with biobased plasticizers derived from epoxidized linseed oil (ELO)," *Compos. Part B - Eng.* 86(1 Feb. 2016), 168-177. DOI: 10.1016/j.compositesb.2015.09.063
- Bledzki, A., Franciszczak, P., Osman, Z., and Elbadawi, M. (2015). "Polypropylene biocomposites reinforced with softwood, abaca, jute, and kenaf fibers," *Ind. Crop Prod.* 70(Aug. 2015), 91-99. DOI: 10.1016/j.indcrop.2015.03.013
- Bouafif, H., Koubaa, A., Perré, P., Cloutier, A., and Riedl, B. (2009). "Wood particle/high-density polyethylene composites: Thermal sensitivity and nucleating ability of wood particles," *J. Appl. Polym. Sci.* 113(1), 593-600. DOI: 10.1002/app.30129
- Cisneros-López, E. O., González-López, M. E., Pérez-Fonseca, A. A., González-Núñez, R., Rodrigue, D., and Robledo-Ortíz, J. R. (2017). "Effect of fiber content and surface treatment

- on the mechanical properties of natural fiber composites produced by rotomolding," *Compos. Interfaces* 24(1), 35-53. DOI: 10.1080/09276440.2016.1184556
- Das, M., and Chakraborty, D. (2008). "Evaluation of improvement of physical and mechanical properties of bamboo fibers due to alkali treatment," *J. Appl. Polym. Sci.* 107(1), 522-527. DOI: 10.1002/app.26155
- Das, M., and Chakraborty, D. (2006). "Influence of alkali treatment on the fine structure and morphology of bamboo fibers," *J. Appl. Polym. Sci.* 102(5), 5050-5056. DOI: 10.1002/app.25105
- Deng, A., Ren, J., Wang, W., Li, H., Lin, Q., Yan, Y., Sun, R., and Liu, G. (2016). "Production of xylo-sugars from corncob by oxalic acid-assisted ball milling and microwave-induced hydrothermal treatments," *Ind. Crop Prod.* 79(Jan. 2016), 137-145. DOI: 10.1016/j.indcrop.2015.11.032
- Dikobe, D., and Luyt, A. (2017). "Thermal and mechanical properties of PP/HDPE/wood powder and MAPP/HDPE/wood powder polymer blend composites," *Thermochim. Acta* 654(10 Aug. 2017), 40-50. DOI: 10.1016/j.tca.2017.05.002
- Ditzel, F. I., Prestes, E., Carvalho, B. M., Demiate, I. M., and Pinheiro, L. A. (2017). "Nanocrystalline cellulose extracted from pine wood and corncob," *Carbohydr. Polym.* 157(10 Feb. 2017), 1577-1585. DOI: 10.1016/j.carbpol.2016.11.036
- Faruk, O., Bledzki, A. K., Fink, H.-P., and Sain, M. (2012). "Biocomposites reinforced with natural fibers: 2000–2010," *Prog. Polym. Sci.* 37(11), 1552-1596. DOI: 10.1016/j.progpolymsci.2012.04.003
- Georgopoulos, S. T., Tarantili, P. A., Avgerinos, E., Andreopoulos, A. G., and Koukios, E. G. (2005). "Thermoplastic polymers reinforced with fibrous agricultural residues," *Polymer Degradation & Stability* 90(2), 303-312. DOI: 10.1016/j.polymdegradstab.2005.02.020
- Guo, J., Zhang, J., Jiang, F., Zhao, S., Su, Q., and Du, G. (2015). "Microporous carbon nanosheets derived from corncobs for lithium–sulfur batteries," *Electrochim. Acta* 176(10 Sept. 2015), 853-860. DOI: 10.1016/j.electacta.2015.07.077
- Haag, K., Padovani, J., Fita, S., Trouvé, J.-P., Pineau, C., Hawkins, S., De Jong, H., Deyholos, M.K., Chabbert, B., and Müssig, J. (2017). "Influence of flax fibre variety and year-to-year variability on composite properties," *Ind. Crop Prod.* 98(April 2017), 1-9. DOI: 10.1016/j.indcrop.2016.12.028
- Hristov, V., and Vasileva, S. (2003). "Dynamic mechanical and thermal properties of modified poly (propylene) wood fiber composites," *Macromol Mater. Eng.* 288(10), 798-806. DOI: 10.1002/mame.200300110
- Huang, L., Wang, H., and Wang, Q. (2015). Influence of β nucleating agent on the crystallization and mechanical properties of PP/wood flour composites," *Polym. Mater. Sci. Eng.* 31(1), 83-87.
- Kaewtatip, K., and Thongmee, J. (2012). "Studies on the structure and properties of thermoplastic starch/luffa fiber composites," *Mater. Des.* 40(Sept. 2012), 314-318. DOI: 10.1016/j.matdes.2012.03.053
- Kang, N., Xu, Y.-Z., Cai, Y.-L., Li, W.-H., Weng, S.-F., Feng, W., He, L.-T., Xu, D.-F., Wu, J.-G., and Xu, G.-X. (2001). "Different states in orthorhombic crystalline phase of high-density polyethylene," *J. Mol. Struct.* 562(1), 19-24. DOI: 10.1016/S0022-2860(00)00721-3
- Leão, R. M., Luz, S. M. d., Araújo, J. A., and Christoforo, A. L. (2015). "The recycling of sugarcane fiber/polypropylene composites," *Mater. Res.* 18(4), 690-697. DOI: 10.1590/1516-1439.321314

- Li, T., and Wolcott, M. (2006). "Rheology of wood plastics melt, Part 2: Effects of lubricating systems in HDPE/maple composites," *Polym. Eng. Sci.* 46(4), 464-473. DOI: 10.1002/pen.20505
- Liu, Q.-y., Yang, F., Sun, X.-f., Liu, Z.-h., and Li, G. (2017). "Preparation of biochar catalyst with saccharide and lignocellulose residues of corncob degradation for corncob hydrolysis into furfural," *J. Mater. Cycles Waste Manage.* 19(1), 134-143. DOI: 10.1007/s10163-015-0392-9
- Luo, Z., Li, P., Cai, D., Chen, Q., Qin, P., Tan, T., and Hui C. (2017). "Comparison of performances of corn fiber plastic composites made from different parts of corn stalk," *Industrial Crops & Products* 95, 521-527. DOI:10.1016/j.indcrop.2016.11.005
- Mao, J., Hou, X., Wang, X., He, G., Shao, Z., and Hu, S. (2015). "Corncob-shaped ZnFe₂O₄/C nanostructures for improved anode rate and cycle performance in lithium-ion batteries," *RSC Adv.* 5(40), 31807-31814. DOI: 10.1039/C5RA04790K
- Na, B., Zhang, Q., Fu, Q., Zhang, G., and Shen, K. (2002). "Super polyolefin blends achieved via dynamic packing injection molding: The morphology and mechanical properties of HDPE/EVA blends," *Polym.* 43(26), 7367-7376. DOI: 10.1016/S0032-3861(02)00637-7
- Nenkova, S., Dobrilova, C., Natov, M., Vasileva, S., and Velev, P. (2006). "Modification of wood flour with maleic anhydride for manufacture of wood-polymer composites," *Polym. Polym. Compos.* 14(2), 185-194.
- Nourbakhsh, A., and Kouhpayehzadeh, M. (2009). "Mechanical properties and water absorption of fiber-reinforced polypropylene composites prepared by bagasse and beech fiber," *J. Appl. Polym. Sci.* 114(1), 653-657. DOI: 10.1002/app.30605
- Panthapulakkal, S., Zereshkian, A., and Sain, M. (2006). "Preparation and characterization of wheat straw fibers for reinforcing application in injection molded thermoplastic composites," *Bioresour. Technol.* 97(2), 265-272. DOI: 10.1016/j.biortech.2005.02.043
- Panthapulakkal, S., and Sain, M. (2007). "Agro-residue reinforced high-density polyethylene composites: fiber characterization and analysis of composite properties," *Composites Part A Applied Science & Manufacturing* 38(6), 1445-1454. DOI: 10.1016/j.compositesa.2007.01.015
- Qiao, M., Ran, Q., Wu, S., and Shen, J. (2009). "Impact of ultraviolet radiation on HDPE and HDPE/STC blends," *Polym. Adv. Technol.* 20(3), 341-346. DOI: 10.1002/pat.1273
- Qu, W.-H., Xu, Y.-Y., Lu, A.-H., Zhang, X.-Q., and Li, W.-C. (2015). "Converting biowaste corncob residue into high value added porous carbon for supercapacitor electrodes," *Bioresour. Technol.* 189(Aug. 2015), 285-291. DOI: 10.1016/j.biortech.2015.04.005
- Xu, Shu-fen. (2011). "Talking about the comprehensive utilization of corncob," *Sci-Tech Inf. Dev. Econ.* 21(17), 174-175. DOI: 10.3969/j.issn.1005-6033.2011.17.074
- Silvério, H. A., Neto, W. P. F., Dantas, N. O., and Pasquini, D. (2013). "Extraction and characterization of cellulose nanocrystals from corncob for application as reinforcing agent in nanocomposites," *Ind. Crop Prod.* 44(Jan. 2013), 427-436. DOI: 10.1016/j.indcrop.2012.10.014
- Song, L.-x., Zhang, P., Yao, N.-n., Song, Y.-z., Kang, M., and Song, K.-p. (2013). "Study on effect of particle diameter and filling quantity of wood flour on mechanical properties of wood-plastics composite," *J. Funct. Mater.* 44(17), 2451-2454. DOI: 10.3969/j.issn.1001-9731.2013.17.003
- Stokke, D. D., and Gardner, D. J. (2003). "Fundamental aspects of wood as a component of thermoplastic composites," *J. Vinyl Add. Technol.* 9(2), 96-104. DOI: 10.1002/vnl.10069

- Sullins, T., Pillay, S., Komus, A., and Ning, H. (2017). "Hemp fiber reinforced polypropylene composites: The effects of material treatments," *Compos. Part B - Eng.* 114(1 April 2017), 15-22. DOI: 10.1016/j.compositesb.2017.02.001
- Tingyun, K., Kezhi, B., and Xiushan, Y. (2007). "Suggestions on the development strategy of bioenergy in China," *Prog. Chem. - Beijing* 19(0708), 1060-1063.
- Tufan, M., and Ayrilmis, N. (2016). "Potential use of hazelnut husk in recycled high-density polyethylene composites," *BioResources* 11(3), 7476-7489. DOI: 10.1016/j.jcis.2005.02.033
- Yan, Y.-H., Li, H.-L., Ren, J.-L., Lin, Q.-X., Peng, F., Sun, R.-C., and Chen, K.-F. (2017). "Xylo-sugars production by microwave-induced hydrothermal treatment of corncob: Trace sodium hydroxide addition for suppression of side effects," *Ind. Crop Prod.* 101(July 2017), 36-45. DOI: 10.1016/j.indcrop.2017.02.024
- Yali, L. (2012). "Effect of coupling agent concentration, fiber content, and size on mechanical properties of wood/HDPE composites," *International Journal of Polymeric Materials & Polymeric Biomaterials* 61(11), 882-890. DOI: 10.1080/00914037.2011.617338
- Zakikhani, P., Zahari, R., Sultan, M., and Majid, D. (2014). "Extraction and preparation of bamboo fibre-reinforced composites," *Matter Des.* 63(Nov. 2014), 820-828. DOI: 10.1016/j.matdes.2014.06.058
- Zhang, L., Xi, G., Yu, K., Yu, H., and Wang, X. (2017). "Furfural production from biomass-derived carbohydrates and lignocellulosic residues *via* heterogeneous acid catalysts," *Ind. Crop Prod.* 98(April 2017), 68-75. DOI: 10.1016/j.indcrop.2017.01.014
- Zhu, X., and Yang, Z. (2010). "A study on irradiated HDPE/sericite composites," *J. Polym. Eng.* 30(8), 447-460. DOI: 10.1515/POLYENG.2010.30.8.447

Article submitted: November 2, 2017; Peer review completed: February 25, 2018; Revised version received and accepted: March 27, 2018; Published: April 2, 2018.
DOI: 10.15376/biores.13.2.3778-3792